ACS APPLIED MATERIALS & INTERFACES
Research Article
www.acsami.org

Aminosilanization Nanoadhesive Layer for Nanoelectric Circuits with Porous Ultralow Dielectric Film

Zhongkai Zhao,[†] Yongyong He,[†] Haifang Yang,[‡] Xinping Qu,[§] Xinchun Lu,[†] and Jianbin Luo*[,†]

[†]State Key Laboratory of Tribology, Tsinghua University, Beijing 100084, China

[‡]Beijing National Laboratory for Condensed Matter Physics, Institute of Physics, Chinese Academy of Sciences, Beijing 100190, China

[§]State Key Laboratory of ASIC & System, Department of Microelectrics, Fudan University, Shanghai 200433, China

ABSTRACT: An ultrathin layer is investigated for its potential application of replacing conventional diffusion barriers and promoting interface adhesion for nanoelectric circuits with porous ultralow dielectrics. The porous ultralow dielectric ($k \approx 2.5$) substrate is silanized by 3-aminopropyltrimethoxysilane (APTMS) to form the nanoadhesive layer by performing oxygen plasma modification and tailoring the silanization conditions appropriately. The high primary amine content is obtained in favor of strong interaction between amino groups and copper. And the results of leakage current measurements of metal-oxide-semiconductor capacitor structure demonstrate that the aminosilanization nanoadhesive layer can block copper diffusion effectively and guarantee the performance of devices. Furthermore, the results of four-point bending tests indicate that the nanoadhesive layer with monolayer structure can provide the satisfactory interface toughness up to 6.7 ± 0.5 J/m^2 for Cu/ultralow-k interface. Additionally, an annealing-enhanced interface toughness effect occurs because of the formation of Cu−N bonding and siloxane bridges below 500 °C. However, the interface is weakened on account of the oxidization of amines and copper as well as the breaking of Cu−N bonding above 500 °C. It is also found that APTMS nanoadhesive layer with multilayer structure provides relatively low interface toughness compared with monolayer structure, which is mainly correlated to the breaking of interlayer hydrogen bonding.

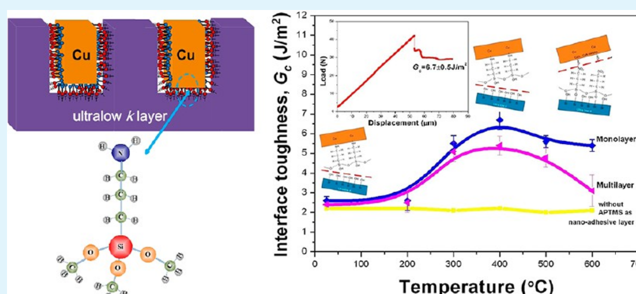

KEYWORDS: *aminosilanization, adhesive, low dielectric, oxygen plasma, diffusion barrier, interface adhesion*

INTRODUCTION

Low dielectric permittivity (k) insulators have been introduced into nanoelectric devices such as integrated circuits,[1,2] high-frequency electronic devices,[3] communication, and packages.[4] The ultralow-k value (∼2.5) can be obtained when nanopores are formed in the carbon-doped silica or SiCOH films that can maintain the reliability after postdeposition curing.[1] However, copper ions can generate and transport readily across the Cu/dielectric interface to cause the performance degradation of nanoelectric devices.[5] Conventional solution is to deposit an ultrathin and conformal noble metal or its nitride layer as an intermediary layer in order to inhibit copper diffusion efficiently. Although the conventional method is effective in most applications, it may not be applicable in the future nanoelectric circuits because such a separate layer (thicker than 5 nm) cannot be a suitable option for nanoscale features (e.g., ∼45 nm).[6] And even International Technology Roadmap for Semiconductors (ITRS) forecasts that the thickness of diffusion barrier will be less than 1 nm by 2021.[7] Therefore, it is extremely necessary and valuable to develop new barrier materials and methods to meet this requirement. Recent investigations have reported molecular nanolayers (MNLs) based on self-assembly with carboxyl-,[8] mercapto-,[9−11] or amino-[8,12−14] functional groups and these studies highlight the fact that the functionalized silane layer can hamper copper diffusion because of the interaction between copper and functional groups. Caro et al. further found that NH_2-self-assembled monolayer (NH_2−SAM) derived from 3-aminopropyltrimethoxysilane is the most promising for Cu diffusion barrier application among a wide variety of silanes with different chain lengths (3−21) and terminal groups (such as CH_3, Br, CN, NH_2, C_5H_4N, and SH).[14]

Stabilizing and enhancing the adhesion of solid−solid interface with molecule-scale adhesive has been investigated systematically.[15] However, there is a big problem with heterointerface adhesion, especially the weakly bonded metal/ceramics and metal/organics interfaces, where interface failures (delamination and cracking) would occur easily during the nanofabrication of circuits. Although a ring-opening-induced toughening method without an additional layer is proposed wonderfully,[16−18] it is only limited to some specific organic substrates and it is also predicted that the blocking properties against copper diffusion could not be improved significantly. In contrast, enhancing Cu/dielectric interface with a nanoscale

Received: March 13, 2013
Accepted: June 9, 2013
Published: June 9, 2013

 © 2013 American Chemical Society

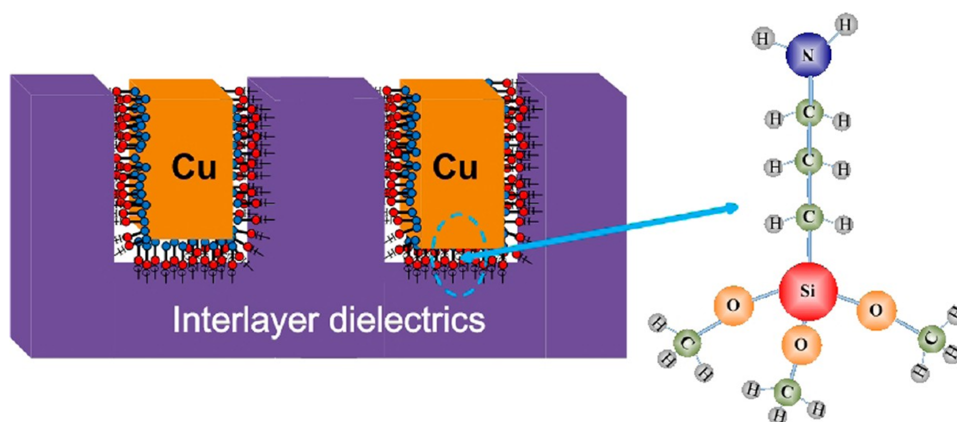

Figure 1. Schematic illustration of the damascene architecture nanofabricated by using 3-aminopropyltrimethoxysilane as a nano-adhesive layer. Damascene architecture is a patterned structure which means inlaying copper within the dielectric trenches to form a metal interconnect in nanoelectric circuits.

Scheme 1. Scheme of the Preparation Process and Interface Adhesion Measurements of the APTMS Silanization Nanoadhesive Layer

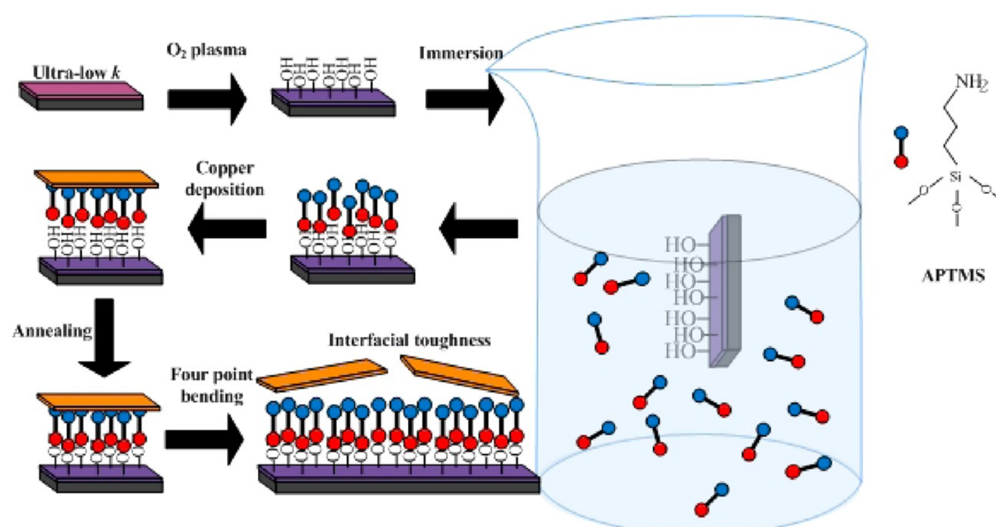

adhesive based on self-assembly or silanization still provides a more attractive alternative and has wider applications. Furthermore, besides excellent heterointerface adhesion, which could match the conventional TaN/Ta sytem,[9,13] it is observed that integrating well-bonded self-assembled MNLs can also provide up to a 4-fold increase in the interface thermal conductance, which has great significance for the thermal reliability of microprocessors and other nanoelectric devices.[19]

Amine-terminated interface/surface has been widely investigated to improve the adhesion in many fields of micro- and nanofabrication.[19,20] It is reported that the system Cu/NH_2−SAM/silica can toughen the interface almost up to an equal value of conventional TaN/Ta system and show no evidence of copper penetration into silica.[13] Accordingly, Figure 1 displays the schematic illustration of damascene architecture nanofabricated by using 3-aminopropyltrimethoxysilane as a nanoadhesive layer in nanoelectric circuits with interlayer dielectrics. In this situation, the fracture failure can occur at three different interfaces, i.e., (i) the interface between the alkoxysilane layer and ultralow-*k* substrate, (ii) the interlayer of the silane film if the polycondensation of multilayer takes place, and (iii) the bonding interface between amino groups and copper. In the first case, in order to enhance the attachment of the alkoxysilane layer on the substrate, considering the hydrophobic nature of porous ultralow-*k* film, which is composed of Si−CH_3 groups oriented outward after curing treatment to suppress the moisture damage of dielectrics, it is demonstrated that oxygen plasma exposure is an effective method to induce −CH_3 abstraction and other chemical changes to form Si−OH groups via a diffusion-dominated mechanism which is widely used in the organosilicate materials.[21,22] In the second case, both of the morphology and the structure of the silanization film are closely related to its coverage and continuity of a barrier against copper diffusion and an adhesion promoter. During the silanization process of alkoxysilane film, the silane precursor is hydrolyzed by a little amount of water contained as a medium, and then attaches to the surface of the hydroxyl substrate covalently. Alternatively, the polycondensation reaction leads to the adsorption of a thick layer and its thickness increment.[12] So, it is very important to tailor the deposition conditions and control the growth of nanoadhesive layers. In the third case, it is well-known that aminosilanization films have been widely utilized in the immobilization of proteins,[23] DNAs[24] and adhesion promotion.[25,26] At the interface between

amino groups and copper, it is necessary to obtain sufficient primary amines on the surface, because these reactive amino moieties can serve as a platform to interact with neighbor molecules and/or atoms. Under the condition of sufficient nucleation sites, copper atoms could attach and be anchored, and thus the adhesion promotion would be achieved.

However, so far, little work has been reported on the deposition of aminosilanization layer on hydrophobic ultralow dielectric film with nanopores, and little is known about the availability and adhesion properties of aminosilanization film as a nanoadhesive layer for the porous ultralow-*k* film/copper interface. Therefore, the purpose of the present paper is to explore the validity to obtain one kind of aminosilanization nanoadhesive layer which can block copper diffusion and promote interface adhesion in nanoelectric circuits.

EXPERIMENTAL DETAILS

Silicon wafers (12 in.) with 500 nm thick porous SiCOH ultralow dielectric thin films (Black Diamond II) were purchased from LAM Corporation, which were prepared by plasma-enhanced chemical vapor deposition (PECVD). The ultralow dielectric ($k \approx 2.5$) thin film has the porosity of about 25% and the average pore size of less than 1 nm. The specimens were cut from the wafer by the size of 10 mm × 20 mm for aminosilanization.

The process including the preparation and adhesion measurements of the APTMS aminosilanization film is shown in Scheme 1. The surface of the dielectric material was modified first by the pure oxygen plasma treatment to bring about hydroxyls on the substrate surface. The resulting material consists of a partially oxidized zone toward the surface and a nonmodified zone toward the silicon substrate. The film was etched using PlasmaLab 80 Plus (Oxford Instruments). The reactor chamber was evacuated to 25 Pa with a mechanical vacuum pump and then purged with etching gas for 1 min. The flow rate of oxygen was set to 30 sccm. The pressure was held constant in the range from 15 to 750 mTorr. The plasma was ignited at 100 W for 1 min. When the plasma was extinguished, the gas continued flowing for an additional 2 min, the reactor was held under the pressure of 187 mTorr, and then opened to the atmosphere. In order to investigate the chemical nature of the prepared surface, Fourier transform infrared (FTIR) absorption spectroscopy was employed on Thermo Fisher Scientific nioclet 6700 in transmission mode. And the thickness measurement of the thin film was performed by an Optrel Multiskop Ellipsometry.

In the experiment, 3-aminopropyltrimethoxysilane (APTMS) and other agents were supplied by Sigma Aldrich. The ultralow-*k* substrate etched by oxygen plasma was immersed in the solution of APTMS using anhydrous toluene as solvent with different concentrations, i.e., 3, 5, and 10 mM, for different time from half an hour to 12 h, respectively. And then the deposited film was rinsed rigorously several times with pure toluene, a mixture of toluene and methanol (1:1 in volume), and pure methanol subsequently. Finally, the wafer was dried with nitrogen flow. The prepared samples were stored under a vacuum (~0.1 Pa) if not used immediately. MFP-3D AFM was used to observe the surface morphology with AC240 silicon tip in the tapping mode.

The macroscopic order and the chemical composition of the prepared aminosilanization film were routinely analyzed using an X-ray photoelectron (XPS) instrument and a water contact angle (WCA) measurement. XPS analysis was carried out by ESCALAB 250Xi with an Al Kα probe beam. The copper film was deposited on the coupons by PVD using RF (~70 nm) and DC magnetron sputtering (~1000 nm) subsequently.

Metal-oxide-semiconductor (MOS) capacitor structures were fabricated by sputter-depositing 500-nm-thick, 1-mm-diameter Cu dots through a shadow mask. We carried out the leakage current measurements using a HP 4278A I−V meter on these MOS capacitors under the electric field with the bias voltage up to a 2 MV/cm.

The adhesion of the film stacks was also measured by four-point bending (FPB) tests on DTS delamination system. Fracture energy (interface toughness) measurements were carried out at a 0.1 μm/s strain rate with 10 × 50 mm^2 symmetric Cu/APTMS/ultralow-*k*/Si coupons. The samples were annealed in a RTP system from 200 to 600 °C for 20 min before the adhesion measurements. The Epotek ND353 epoxy resin used here was cured for 12 h at 50 °C.The dice and notch processes were carried out with the same 10-μm width. Before the FPB tests, the specimens were annealed for 30 min at 70 °C in order to remove the absorbed moisture. Afterward, XPS analysis on each side of the fractured interface gives the evidence to analyze the failing interface.

RESULTS AND DISCUSSION

Surface Modification by Oxygen Plasma Treatment. The ultralow dielectric film used in our experiments is hydrophobic with the water contact angle (WCA) of about 100.4° because of the generation of alkyl groups and pore sealing after ultraviolet (UV) curing treatment.[1] The WCA and the surface roughness of the ultralow dielectric materials before and after pure oxygen plasma surface modification are shown in Figure 2. The results show that WCA decreases with the

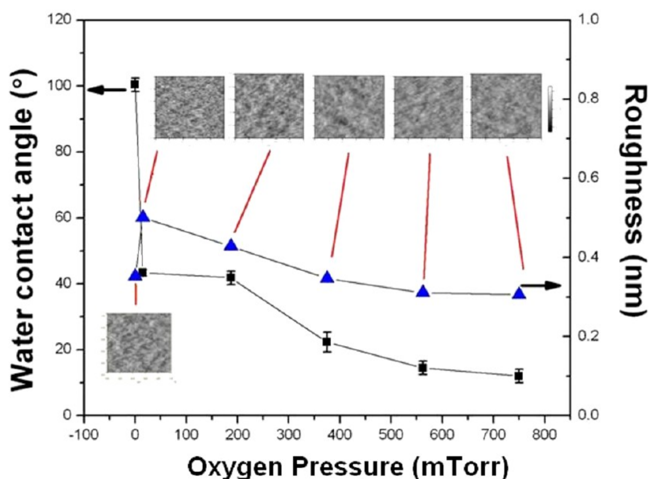

Figure 2. Water contact angle and roughness of the sample surfaces before and after oxygen plasma treatment under different oxygen pressures. The AFM image is on a 500 nm scale.

increment of oxygen pressure and the lowest contact angle (WCA~15°) can be obtained under the oxygen pressure of 750 mTorr. Furthermore, to detect the chemical states, we used FTIR spectra of the ultralow-*k* film after the oxygen plasma modification under different oxygen pressure as shown in Figure 3. It is evident that larger pressure can enhance the intensity of shakeup peak with wave numbers from 3600 to 3100 cm^{-1}, corresponding to Si−OH bonds,[5] which would be helpful for the attachment of methyl groups of APTMS molecules to the ultralow dielectric substrate. The hydroxylation reaction of the pure oxygen plasma treatment is given as follows,

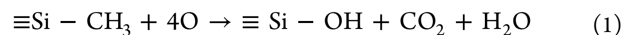

$$\equiv Si - CH_3 + 4O \rightarrow \equiv Si - OH + CO_2 + H_2O \quad (1)$$

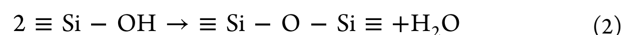

$$2 \equiv Si - OH \rightarrow \equiv Si - O - Si \equiv + H_2O \quad (2)$$

where ≡Si denotes Si bonded by three lattice O. It is also proposed that some portion of Si−OH would further react by the reaction 2. Thus, the reaction would evolve H_2O and CO_2. Note that the only reaction that changes the structure is at the site of the original Si−CH_3.[27] It was reported that gas plasma exposure not only could introduce hydroxyls into the surface of

dx.doi.org/10.1021/am4009192 | ACS Appl. Mater. Interfaces 2013, 5, 6097−6107

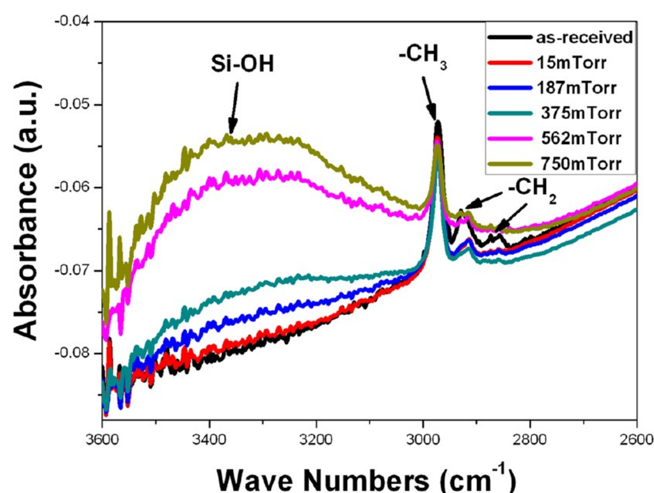

Figure 3. FTIR spectra of the ultralow-*k* thin film before and after oxygen plasma treatment under different oxygen pressures.

substrates but also would usually roughen the smooth surface of polymers.[28,29] However, in our experiment, it is amazing that although the surface is roughened up to R_a = 0.50 nm under the oxygen pressure of 15 mTorr, smoother surface is obtained by increasing the oxygen pressure, and even the roughness goes down to 0.30 nm, which is a little smaller than that of the original ultralow-*k* film (R_a = 0.35 nm). Considering that the mechanism of plasma reaction is fairly complex, it seems that the free radicals strongly modify the chemical bonds of Si−CH_3 and the active oxygen-ion bombardment is not dominant effect under the high pressure during pure oxygen plasma exposure in our experiment. Above all, the smooth and hydrophilic surface with a great amount of hydroxyls gives help to the deposition and growth of the APTMS silanization layer.

Deposition Parameters Affecting APTMS Silanization on Ultralow-*k* Film. The silanization process developed to attach the APTMS molecules to the ultralow-*k* substrate involves the hydroxylation by oxygen plasma treatment followed by the immersion in solution phase as shown in Scheme1.

The high-resolution XPS spectra of C1s and N1s for the different samples are shown in Figure 4. In the C1s core level XPS spectra, before APTMS deposition, an overwhelming peak centered at around 284.6 eV is principally attributed to C−Si or C−C bondings.[25] It is seen that after the oxygen plasma exposure, there is an extra C−O component at higher binding energy of 286.2 eV,[25] and carbonyl carbon (COO) peak with a wider binding energy range from 288 to 290 eV,[30−32] which is ascribed to the incomplete hydroxylation reaction of alkyl groups at the ultralow-*k* surface. During silanization, APTMS molecules could be hydrolyzed at the methoxy end groups, and then condense with the surface hydroxyls to produce siloxanes (Si−O−Si). Besides the presence of C−C or C−Si component at lower binding energy, C−N component at the higher binding energy (286.1 eV) which might originate from the C atoms bonded to the N atoms (C-NH_2)[33,34] is identified after APTMS silanization.

After the attachment of APTMS molecules to the substrate, amino groups would be oriented outward which are detectable as shown in N1s core level spectrum. The peak at 398.8 eV[25] corresponds to the primary amine (the primary amine content is established as the percentage of −NH_2 component in the XPS N1s spectrum). Nevertheless, some amino groups may

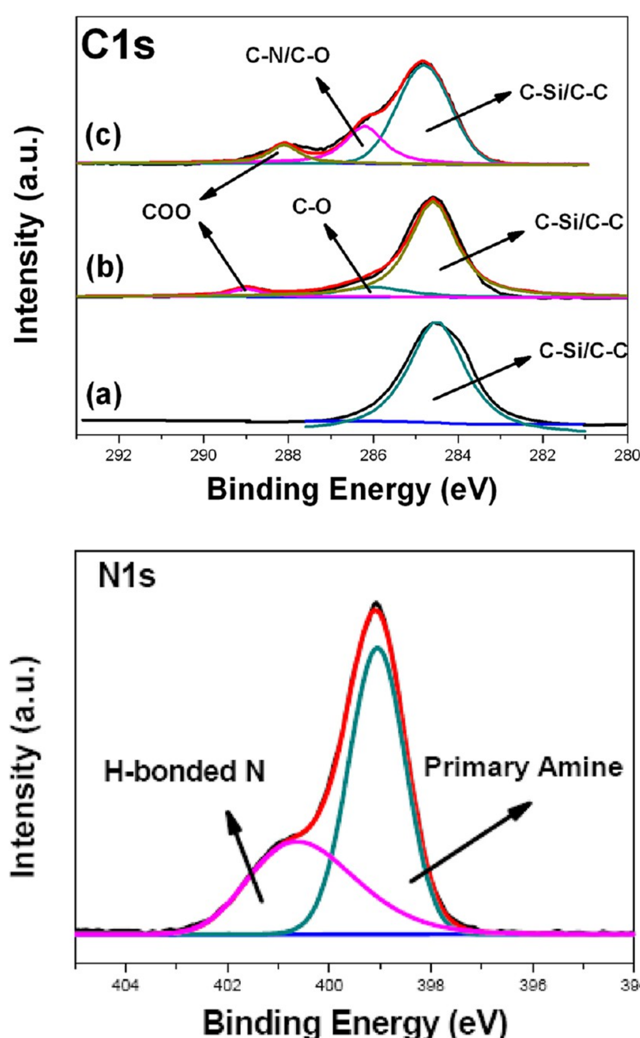

Figure 4. XPS C1s spectra (on the top) for (a) as received, (b) after oxygen plasma exposure, and (c) after APTMS silanization. And XPS N1s spectrum (on the bottom) after APTMS silanization.

also undergo hydrogen bonding with each other or hydroxyls of the substrate, which is demonstrated by the presence of the shoulder at 400.7 eV.[25,33]

Scheme 2 displays APTMS hydrolysis followed by condensation reaction in solution phase and APTMS attachment on hydroxyl-terminated ultralow-*k* surface. At the beginning of ATPMS silanization in solution phase, the hydrolysis could drive the attachment of ATPMS molecules to the hydroxyl-terminated substrate. This process depends on the amount of water which would absorb on the substrate as reaction medium or catalysis in the system. But overabundance of water will cause the excess polymerization in solution phase and yield polycondensed layers on the substrate, whereas the deficiency of water will result in the formation of incomplete monolayer.[35] Alternatively, during the hydrolysis of APTMS molecules, a dimerization reaction may occur eventually leading to the formation of oligomers which can be absorbed at the substrate to form a thick polycondensed layer ultimately. To minimize this phenomenon, we should use the low concentration of ATPMS and tailor it precisely and appropriately. After the formation of well-organized APTMS monolayers through covalent bonding, the bilayer could be formed through hydrogen bonding. And then a self-replicating

Scheme 2. Schematic Illustration of (a) APTMS Hydrolysis Followed by Condensation Reaction in Solution Phase and (b) APTMS Attachment on Hydroxyl-Terminated Ultralow-*k* Surface

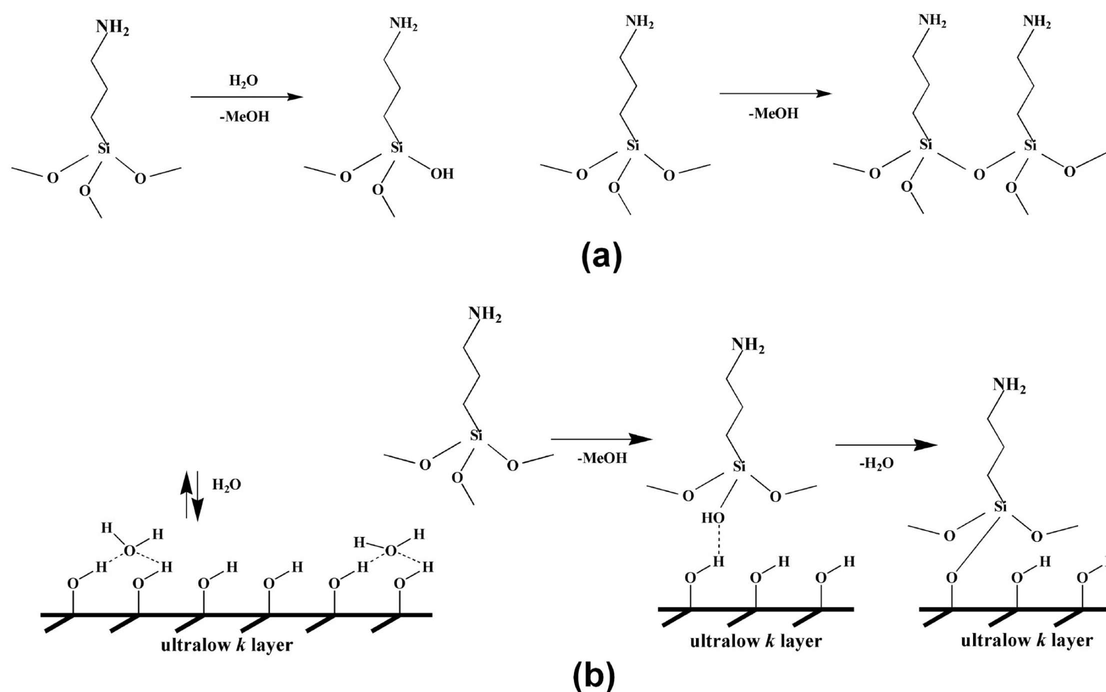

reaction takes place and the APTMS multilayers would be formed.[36]

All the attachment kinetics and reaction processes above are closely related to the deposition parameters such as solute concentration, deposition time, water content, and temperature. Next, we will investigate the effects of these parameters on the attachment kinetics of APTMS silanization.

ATPMS Concentration. The effects of APTMS concentration on the deposition of aminosilanization films were investigated by immersion for 2 h. AFM images and the surface roughness are shown in Figure 5. It is seen that when the concentration is 3, 5, and 10 mM, the surface roughness R_a is 0.63, 0.94, and 2.42 nm, respectively. It indicates that higher concentration cannot contribute to the formation of uniform films with smooth topography. When the lower APTMS concentration is utilized, the ATPMS molecules opt to assemble mainly in the form of monomers, dimers in the bulk solution. However, when the concentration is higher, APTMS molecules will exhibit less orientation or disordered growth and aggregate to form large oligomers in the solution before the attachment to the hydroxyl-terminated ultralow-*k* substrate. Meanwhile, it is observed that when the APTMS concentration is 3, 5, and 10 mM, the primary amine content is 69.9, 43.4, and 21.1%, respectively. The lower concentration can yield the higher content of primary amines. As discussed above, higher APTMS concentration in the solvent means that the amino groups will undergo more interaction with each other, are more likely to aggregate into large oligomers through hydrogen bonding and as a result, many primary amines may be lost.

Water as the Deposition Medium. Figure 6 shows the AFM images of APTMS deposited on the ultralow dielectric substrate with different water contents, which are 0.1 and 1 wt % water as medium or catalyst, and without water controlled by anhydrous $MgSO_4$ powder, respectively. It is clear that anhydrous environment means that water is not located at the hydroxyl surface when APTMS clusters are absorbed, uncontrolled and disordered growth would occur and the surface becomes significantly rough (R_a = 6.41 nm). A trace amount of water (0.1 wt %) is favorable for obtaining a smooth topography with the roughness of 0.39 nm. However, the water content should not be overabundant leading to the adsorption of a thick polycondensed layer on the substrate as mentioned previously.[35] The higher water content of 1% results in the rougher morphology (R_a = 2.84 nm) because APTMS molecules may polymerize rapidly to form large oligomers in the solution and finally deposit on the substrate surface. Therefore, a trace amount of water (~0.1 wt %) is required as the medium or catalyst for the uniform deposition of the APTMS silane on the ultralow-*k* substrate, which is similar to the silica substrate.[25]

Deposition Time. By using 3 mM solution in toluene with 0.1 wt % water content at room temperature (RT), the content of primary amines varies with deposition times as shown in Figure 7. It is found that the immersion for about 6 h can provide the highest primary amine content. In the solution, there is a competition between the amino groups and the methoxy groups of APTMS molecules that could interact with the hydroxyl-terminated substrate. When the immersion time is short, more methoxy groups predominately attach the substrate with hydrogen bonding interaction which causes the amino groups outward indicated by the increase of primary amine contents. However, APTMS molecules assemble mainly in the form of oligomers in the solution accompanying with the loss of amino groups when increasing the immersion time. After silanization, the uniform surface becomes a little more hydrophobic (WCA ≈ 25°) compared with that of the oxygen plasma treated sample, which can prevent further moisture uptake.

Moreover, the thickness of the ultrathin films was also measured by ellipsometry as illustrated in Figure 7. By controlling the deposition conditions, the APTMS silane films, deposited for half an hour and 2 h with the thickness

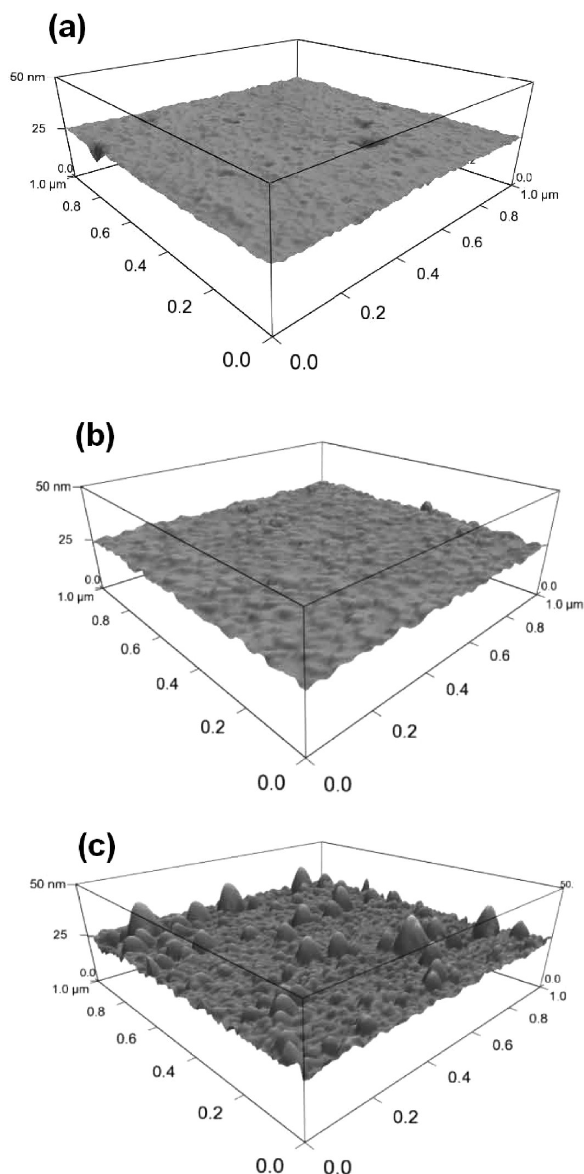

Figure 5. AFM images of the APTMS deposited on the ultralow-k film with different concentrations: (a) 3 mM, R_a = 0.63 nm; (b) 5 mM, R_a = 0.94 nm; (c) 10 mM, R_a = 2.42 nm.

of about 1.5 ± 0.3 and 3.4 ± 0.5 nm, respectively, were chosen because these films could meet the demands of sub-5 nm thickness as a diffusion barrier in nanoelectric circuits. Chauhan et al reported that the thickness of the grafted APTMS layer was 7 Å which was nearly equal to the theoretical length of APTMS molecule.[36] But it was also reported that the experimental value of ellipsometry measurement for a uniform self-assembled monolayer is about 1.3 nm on silica.[37] The difference could arise from several factors, e.g., different solution concentrations, different conditions of the substrate surface, different head groups of silane molecules, and different ambient conditions when APTMS silanization reaction takes place. Therefore, it could be concluded that the amino-silanization films deposited for half an hour and 2 h would probably exhibit monolayer and multilayer structure, respectively. Moreover, it must be noted that, because the uniform and defect-free deposition of silanization films are required to avoid the partial-monolayer structure, to a certain extent, it is

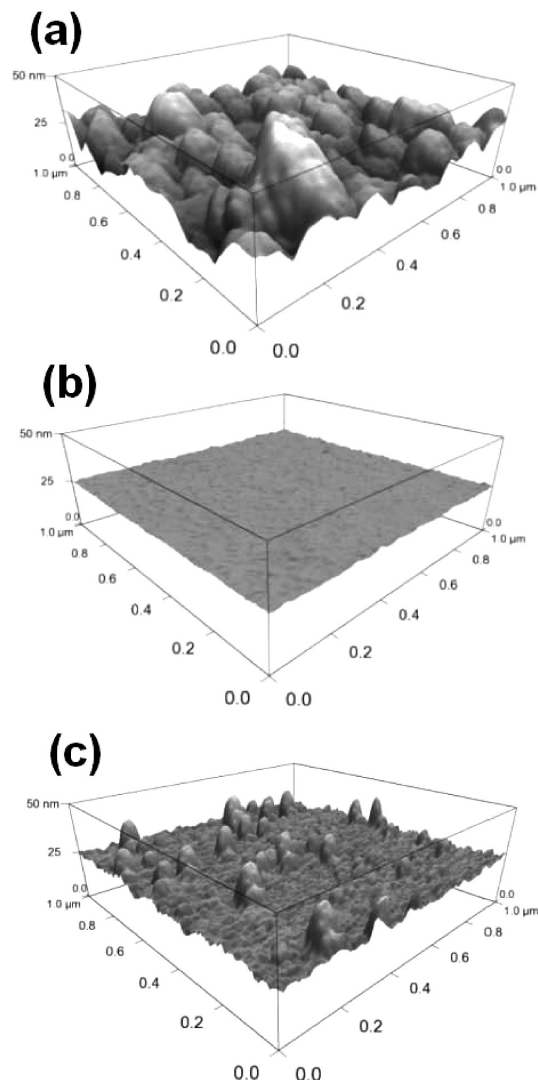

Figure 6. AFM images of APTMS silanization on ultralow-k substrate with different water contents: (a) without water, R_a = 6.41 nm; (b) with 0.1 wt % water content, R_a = 0.39 nm; (c) with 1wt % water content, R_a = 2.84 nm.

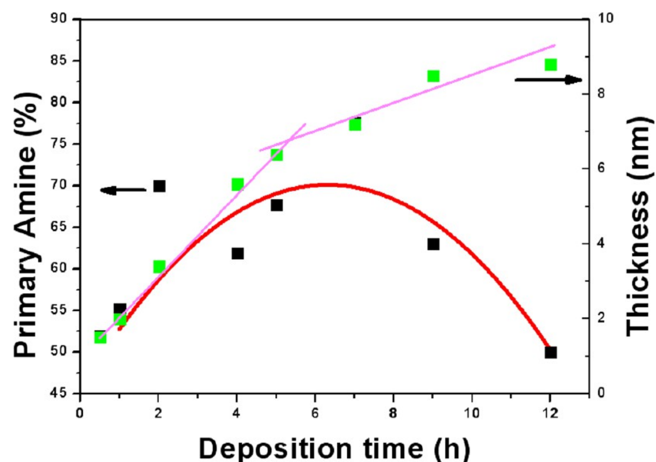

Figure 7. Primary amine content and thickness as function of deposition time.

inevitable to obtain multilayer-structure in order to guarantee the blocking properties against copper diffusion.

Curing Temperature. Postdeposition curing can not only remove the residual solvent but also affect the chemical states of the surface of APTMS silanization film. The samples that are deposited for 0.5 h in 3 mM solution were prepared for thermal curing at different temperatures for 10 min in the air. The chemical bonding states of the APTMS films before and after curing were examined using XPS as shown in Figure 8. It can be observed that when the films are cured at the temperatures below 150 °C, the shoulder of the H-bonded N shrinks which confirms that there is a conversion from the H-bonded amines to the primary amines which leads to the increase of the primary amine content from 52.3% to 77.5% resulting from thermal-induced breakup of hydrogen bonds between amino groups and hydroxyls of ultralow-*k* substrate. However, the curing temperature should not be too high above 250 °C, otherwise a large number of amines will react with CO_2 in the ambient atmosphere and thus some primary amine groups would be lost significantly to form −NHCOOH groups that are thermally sensible and can decompose to amines and CO_2 upon excessive heating finally.[25]

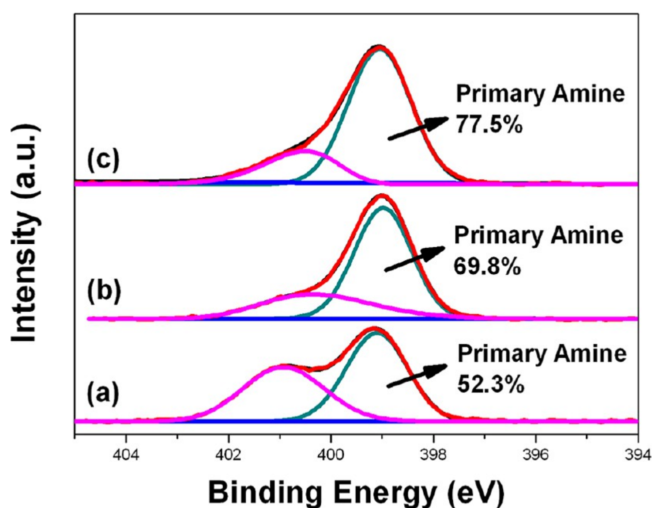

Figure 8. XPS N1s spectra and primary amine contents at different postdeposition curing temperatures: (a) RT, (b) 100 °C, (c) 150 °C.

Blocking Properties against Copper Diffusion. Excellent blocking properties against copper diffusion of ATPMS monolayer deposited on silicon and silica have been confirmed by sheet resistance[14] and direct observation through transmission electron microscopy.[13] In our experiment, the leakage current measurements of MOS structure with APTMS silanization layer on the ultralow dielectric substrate after annealing at 200 °C were carried out under different voltages. The results are shown in Figure 9. For the APTMS silanized sample with monolayer structure as a nanoadhesive layer, the leakage current is reduced significantly compared with that of the sample without the aminosilanization layers. It is evident that aminosilanization layer can effectively block the diffusion of copper atoms or ions into the porous ultralow-*k* film and avoid dielectric breakdown. The reduction in leakage current may be attributed to the formation of Cu−N bonds which plays an important role in diffusion barrier. It is also revealed that copper attached aminosilanization films through a probable bonding (covalent or chelative bonding interaction) could hamper the transportation of Cu ions into the porous ultralow-*k* film.[8,38] In addition, APTMS molecules with a smaller molecular length (∼0.7 nm) compared with the pore size (∼1 nm) of the ultralow-*k* film, would provide the role of sealing pores partially. Regarding the temperature effects on the reliability of aminosilanization layers in the application of devices, Mikami et al. reported that an estimated lifetime was longer than ten years at the device operation temperature of 120 °C.[38] Although these results were based on Cu/silica interconnect, the reliability of APTMS silanization layer for ultralow-*k* substrate is expectable, which will be explored in our future work.

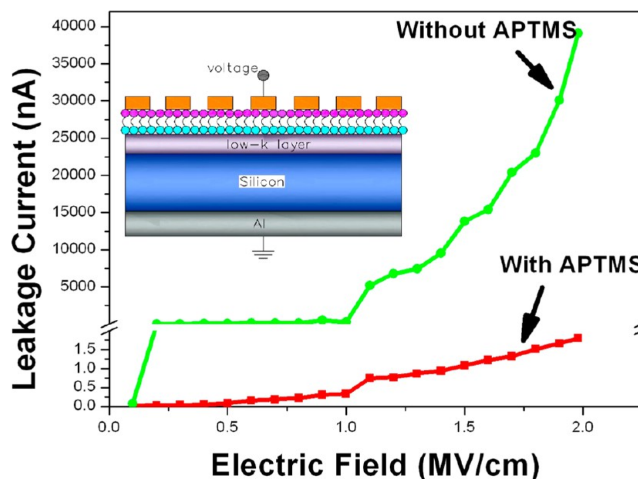

Figure 9. Leakage current measurements of MOS structure with and without APTMS monolayer as a nanoadhesive layer.

Adhesion Properties for Cu/Nanoadhesive Layer/Ultralow-*k* Film System. To determine the fracture interface between the Cu film and the ultralow-*k* substrate, we performed four-point bending (FPB) tests in our investigation. As is well-known, four-point bending test is a standard method to quantitatively measure G_c, i.e., the interface adhesion toughness, which is commonly characterized by the critical strain energy release rate defined as eq 3

$$G = \frac{21(1 - \nu^2)M^2}{4Eb^2h^3} \quad (3)$$

where the bending moment $M = PL/2$, with P being the load and L the space between the inner and the outer loading lines, b is the beam width, h is the half thickness, and E and n are the elastic modulus and Poisson's ratio of the bulk substrate, respectively.[39]

The experimental results of the interface toughness measurements at different temperatures are shown in Figure 10. It is so amazing that the hydroxylation of ultralow-*k* substrate after pure oxygen plasma surface modification can provide the strong bonding between the methoxyl groups of APTMS and hydroxyls of ultralow-*k* substrate surface after silanization reaction. It can be seen that the interface is toughened with the increment of annealing temperature below 400 °C, which demonstrates an annealing-enhanced effect for the Cu/APTMS/ultralow-*k*/Si film stacks. The strongest interface toughness can reach about 6.7 ± 0.5 J/m^2 at 400 °C for the APTMS monolayer as nanoadhesive layer and 5.4 ± 0.4 J/m^2 at 400 °C for the APTMS multilayer as nanoadhesive layer, whereas the toughness can reach 2.6 ± 0.2 and 2.2 ± 0.2 J/m^2 at the room temperature (RT) for the monolayer and the multilayer structure, respectively. In contrast, without APTMS as adhesive, the stacks exhibit an average interface toughness of

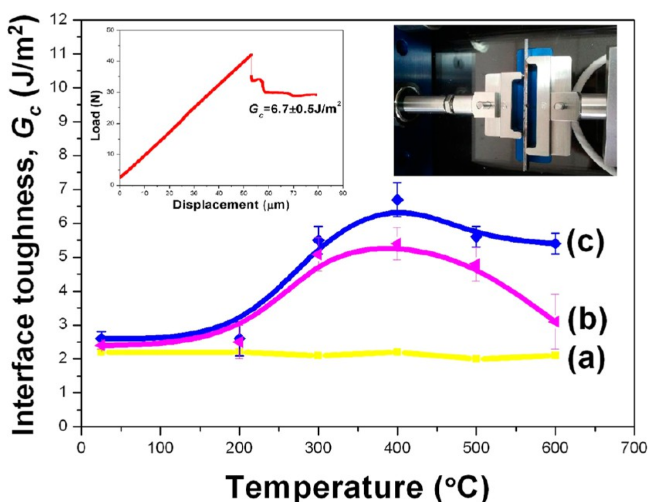

Figure 10. Interface toughness values G_c (J/m^2) at different temperatures: (a) Cu/ultralow-*k*/Si film stacks; (b) Cu/APTMS/ultralow-*k*/Si film stacks with APTMS multilayer as nanoadhesive layer; (c) Cu/APTMS/ultralow-*k*/Si film stacks with APTMS monolayer as nanoadhesive layer.

$G_c \approx 2.2 \pm 0.3$ J/m^2 and no observable change of the interface toughness appears during annealing process.

It is well-known that there is a critical interface adhesion energy (i.e., about 5 J/m^2) that could prevent interface from delamination and crack during the fabrication of nanoelectric circuits.[2] In our work, the APTMS silanization nanoadhesive layer provides the satisfactory adhesion strength up to 6.7 ± 0.5 J/m^2, which is close to that of commercial TaN/Ta system (7.5 J/m^2).[13] Therefore, it can be expected that the damascene structure using APTMS silanization nanoadhesive layer as shown in Figure 1 could survive from mechanical damage during nanofabrication, and such a nanoadhesive layer could have the potential application in the next generation of nanoelectric circuits.

Moreover, at the temperatures below 500 °C, annealing-induced interface toughness is observed in accordance with those of Cu/MPTMS/SiO_2/Si and Cu/APTMS/SiO_2/Si film stack system. In the Cu/MPTMS/SiO_2/Si system, it was explained that the adhesion enhancement of interface was mainly attributed to irreversible MPTMS dehydration.[9] And in the Cu/APTMS/SiO_2/Si film stack system, with the similar molecular blackbone, the formations of both Cu−N bonds and siloxane bridges due to the dehydration of Si−OH made a great contribution to the enhancement of interface toughness up to 600 °C.[13]

However, above 500 °C, in our experiment, it should be paid close attention to the phenomenon that an annealing-induced weakening of interface adhesion for the samples takes place, which means that there might be another failure mechanism for the Cu/APTMS/ultralow-*k*/Si film stack system at the high temperatures.

To determine the fracture interfaces, we first performed the survey scanning XPS detection of fracture surfaces. For the APTMS monolayer as a nanoadhesive layer, on the copper fracture surface, the survey XPS spectra show the peaks of C and O with a weak N signal besides the prominent signal of Cu substrate, while on the ultralow-*k* fracture surface, the survey XPS spectra show the obvious presence of O, N and C with almost no detectable trace of Cu. And, for the APTMS multilayer as a nanoadhesive layer, on the ultralow-*k* fracture surface, there is almost no difference in the detected elements from the APTMS monolayer condition. However, on the copper fracture surface, the survey spectra display that the elements of C, O, Cu, N, and Si are detected clearly and the intensity of N peak is much stronger than that of the APTMS monolayer.

It is mentioned previously that the APTMS molecules would penetrate into the pores of the ultralow-*k* substrate and the role of sealing pores is achieved because they have molecular diameter of about 0.7 nm, which is smaller than the pore size (∼1 nm) of the ultralow-*k* films, which is proved by the no observable change of I_N/I_{Si} ratio from angle resolution XPS (ARXPS) analysis of ultralow-*k* fracture surface (not shown here). These results are also in agreement with the silanization results of mesoporous silica films.[40]

The XPS N1s, Si2p$_{3/2}$, and Cu2p$_{3/2}$ core level spectra from the Cu fracture surfaces for APTMS monolayer as nano-adhesive layer are shown in Figure 11. At the room temperature and 400 °C, the N1s peak consists of two components, i.e., primary amine and amide-N components appearing at 398.8 eV[25] and 400.1 eV,[33,41] respectively. It is also observed that annealing can result in the loss of primary amine contents and the increment of amide-N contents indicating that there is a thermodynamic transformation. However, the excessive heat treatment up to 600 °C causes the oxidization of amino groups which can be concluded by the presence of additional distinct peak assigned to nitro groups at the range from 405 to 410 eV.[42]

In the Si2p spectra for the Cu fracture surfaces, it is seen that the peak at around 102.2 eV corresponding to C(H)−Si−O_3 groups[21,43] is present, suggesting the fracture occurs at the APTMS/ultralow-*k* interface. In contrast, this signal of Si 2p disappears completely when the temperature is elevated up to 600 °C, suggesting that the interface failure tends to occur at the Cu/APTMS interface.

In the Cu2p XPS core level spectrum for the Cu fracture surfaces, at the room temperature and 400 °C, the peak at 934.2 eV assigned to Cu(II) peak along with a shakeup peak at much higher binding energies (939−944 eV)[44,45] attributed to the formation of Cu−N bonding from Cu/APTMS interface appears besides the presence of the bulk Cu(0) peak at the lower binding energy of 932.4 eV.[45] It is notable that the intensity ratio of $I_{CuN}/I_{Cu(0)}$ decreases and the shakeup peak shrinks at the temperature of 400 °C indicating that annealing hampers the formation of Cu−N bonding. When the temperature is elevated up to 600 °C, the shakeup peak shrinks dramatically and almost disappears. The Cu2p$_{3/2}$ main peak broadens and extends over a wide energy range from 931 to 935 eV. The deconvolution of this peak is done with several components as shown in the inset picture of Cu2p$_{3/2}$ XPS spectrum, i.e., Cu(0) subband centered at 932.4 eV, Cu(II) component from CuO at 933.6 eV[44] and Cu(II) component from CuN at 934.2 eV. Admittedly, the amount of CuO is definitely overestimated because of the additional oxidization during the transferring from the air to the XPS chamber, and thus in our experiment the samples are carefully kept in the vacuum and etched slightly before XPS detections.

According to all the analysis of XPS spectra for the fracture surfaces, it makes sense that the fissure occurs at the APTMS/ultralow-*k* interface below 500 °C. It is known that the amount of oxygen is located at or near the amino groups in amine-terminated self-assembled monolayers detected by XPS, which is explained by the hypotheses of the oxidization of nitrogen

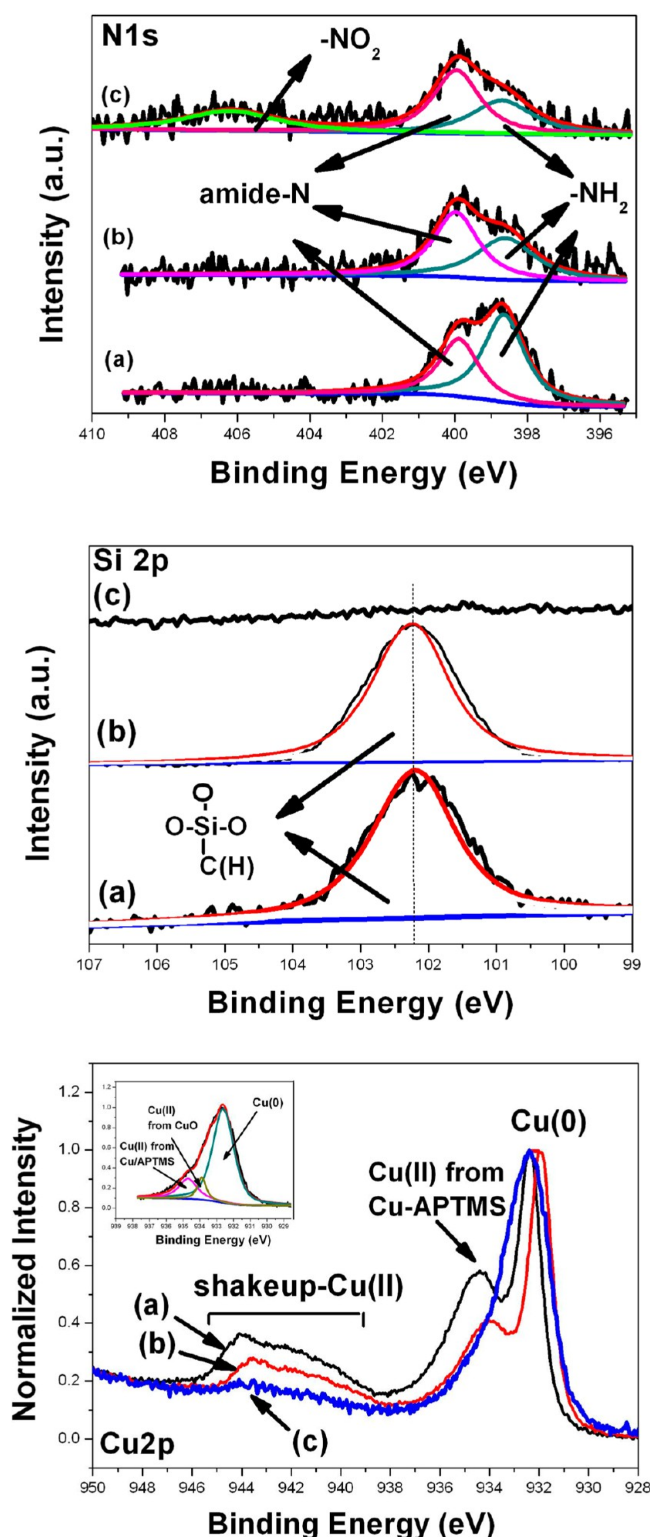

Figure 11. N1s, $Si2p_{3/2}$, and $Cu2p_{3/2}$ XPS spectra of the Cu fracture surfaces for APTMS monolayer as nanoadhesive layer: (a) RT; (b) 400 °C; (c) 600 °C. The deposited copper is mainly in the metallic state. Inset: Zoom on the $Cu2p_{3/2}$ region at the range from 928 to 938 eV for the Cu fracture surface at 600 °C.

and carbon species and the coverage of oxygen containing coadsorbates.[46−48] The presence of oxygen can catalyze the dissociation reaction of $-NH_2$ to −NH, which is nearly thermally neutral or endothermic ($\Delta E[NH_2(a) + O(a) \rightarrow NH(a) + OH(a)]$) = +6 kJ/mol) by thermodynamic calculation.[49] At the Cu/APTMS interface, the reaction between Cu and N atoms takes place in the formation of interfacial complexes due to the donor−acceptor interaction which is strongly confirmed by the detection of Cu2p XPS spectra in Figure 11. Annealing at the elevated temperature from 200 to 400 °C can offer the energy contribution or the driving force to facilitate the loss of hydrogen atoms from amine groups, and thus the consecutive reaction between Cu and N atoms becomes thermodynamically favorable which could make a great contribution to toughening the Cu/APTMS interface. Meanwhile, the dehydroxylation between APTMS and hydroxyls on the ultralow-*k* substrate, which can form strain-relaxed siloxane bridges (Si−O−Si), can also toughen the interface above 300 °C.[9] Therefore, both of the formations of siloxane bridges and Cu−N bonding are critical to toughen the interface below 500 °C.

However, in the presence of oxygen, the dissociation reaction of -NH to nitrogen is exothermic ($\Delta E[NH(a) + O(a) \rightarrow N(a) + OH(a)] = -47$ kJ/mol) according to thermodynamic calculation results.[49] So, excessive heating at the higher temperature above 500 °C can suppress the transformation from -NH to nitrogen and the formation of Cu−N bonding thermodynamically. And the formed Cu−N bonds are prone to breaking at such high temperatures. Besides, the oxidization reaction of amino groups could also take place to produce nitro compounds and the oxidization of Cu to form cupric oxide can further deteriorate the interface, which is supported by the XPS detection in Figure 11. In spite of the irreversible dehydration at the APTMS/ultralow-*k* interface, i.e., the formation of strain-relaxed siloxane bridges that do not revert to silanol groups upon cooling,[9,50] the Cu/APTMS interface is weakened significantly due to the oxidization of amines and copper as well as the breaking of Cu−N bonding. As a result, it is found that the interface toughness for the Cu/APTMS/ultralow-*k* system decreases when the temperature is elevated above 500 °C

The scheme of the fracture mechanism based on APTMS monolayer as nanoadhesive layer between copper and porous ultralow-*k* film is summarized in Figure 12.

When the APTMS multilayer acts as nanoadhesive layer, which is formed because of vertical polymerization favored by hydrogen bonding interaction with relatively low bonding energy (10−40 kJ/mol),[51] although Cu−N bonding and siloxane bridges give help to the interface enhancement during annealing, hydrogen bonding among APTMS molecule interlayers would not suffer from heating and be easily broken so that the fracture opts to occur at the interlayer interface, which is concluded by the presence of the intensive and distinguishable N1s peak with amine components at both of the Cu and ultralow-*k* fracture surfaces during annealing. As a result, the APTMS multilayer nanoadhesive layer exhibits lower macro interface toughness compared with the APTMS monolayer nanoadhesive layer as shown in Figure 10. It seems that ultrathin nanoadhesive layer (monolayer structure) could provide stronger interface adhesion than thicker one (multilayer or polycondensed layer) in the application of nanoelectric circuits. And this phenomenon will be investigated in our next work.

All the explanation above is mainly based on the chemical bonding states. However, the experimentally measured fracture toughness is influenced by a number of other factors such as molecular stretching, lateral molecular interactions, plastic

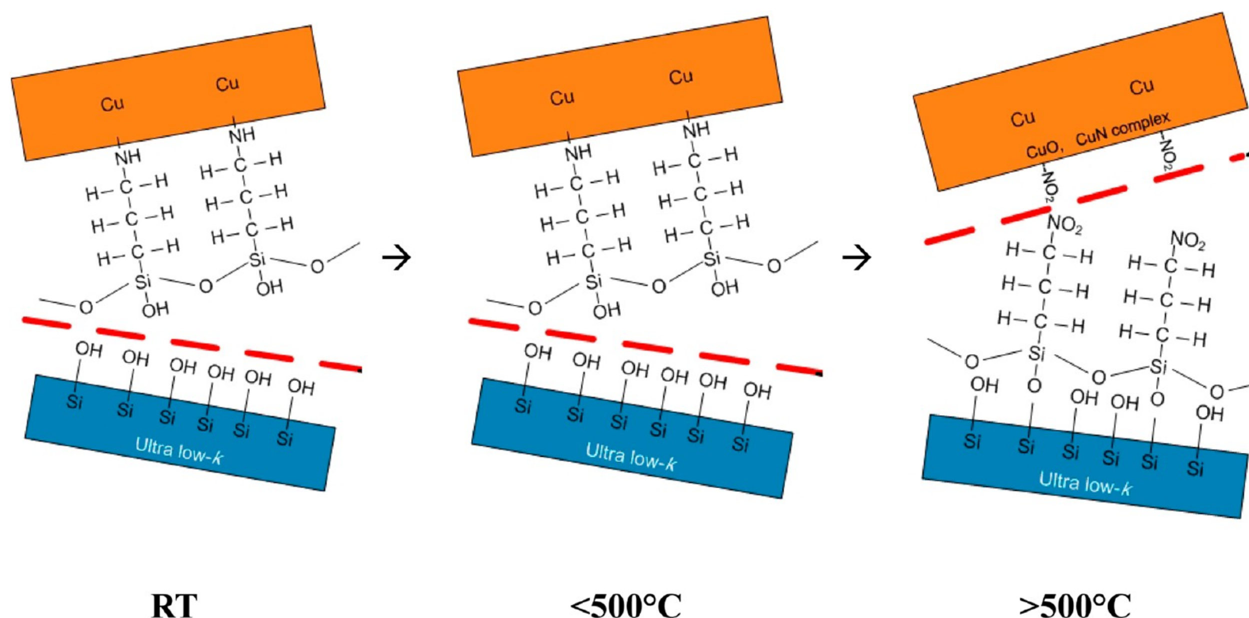

Figure 12. Scheme of the fracture mechanism based on APTMS monolayer as nanoadhesive layer between copper and porous ultralow-*k* film (red dotted line denotes the fracture interface.).

energy dissipation in adjacent films, grain growth, and texture of copper films.[9,52]

In the next investigation, we will try to carry out the deposition of ultrathin nanoadhesive layer on patterned wafers with less than 32-nm-wide trenches and concentrate our attention on the mechanism of bonding between copper and amino groups.

■ CONCLUSIONS

In this paper, the preparation process, block, and interface adhesion properties of the APTMS silanization nanoadhesive layer are investigated for nanoelectric circuits with porous ultralow dielectric film. Oxygen plasma surface modification can bring about a substantial amount of hydroxyl groups on the ultralow-*k* film by increasing the oxygen pressure in the chamber. It is found that the primary amine content can reach up to 77.5% in favor of strong interaction between amino groups and copper atoms. A uniform and continuous layer is obtained by optimizing the deposition conditions. The leakage current measurements of MOS structure indicate that the aminosilanization layer can block copper diffusion effectively and eliminate the degradation of devices. Moreover, the APTMS silanization nanoadhesive layer provides a satisfactory interface toughness up to 6.7 ± 0.5 J/m^2 for Cu/dielectric interface. An annealing-enhanced effect of interface adhesion is observed due to the dehydration of APTMS with the hydroxyls of substrate and Cu−N bonding below 500 °C. However, above 500 °C, the interface is weakened, which is ascribed to the oxidization reactions of amines and copper as well as the breaking of Cu−N bonding. In addition, it is also found that APTMS nanoadhesive layer with multilayer structure provides lower interface toughness than that of monolayer structure, which is mainly correlated to the breaking of interlayer hydrogen bonding.

■ AUTHOR INFORMATION

Corresponding Author

*E-mail: luojb@tsinghua.edu.cn. Tel: 86-10-62781385.

Notes

The authors declare no competing financial interest.

■ ACKNOWLEDGMENTS

We thank Ms. Xiaomeng Zhang and Mr. Xu Wang from Fudan University for the help of four-point bending tests. The work was financially supported by the National Natural Science Foundation of China (Grants 51027007 and 51021064) and the State Key Development Program for Basic Research of China (Grant 2009CB724201).

■ REFERENCES

(1) Volksen, W.; Miller, R. D.; Dubois, G. *Chem. Rev.* **2010**, *110*, 56−110.

(2) Maex, K.; Baklanov, M. R.; Shamiryan, D.; Iacopi, F.; Brongersma, S. H.; Yanovitskaya, Z. S. *J. Appl. Phys.* **2003**, *93*, 8793−8841.

(3) Spencer, T. J.; Osborn, T.; Kohl, P. A. *Science* **2008**, *320*, 756−757.

(4) Meador, M.; Wright, S.; Sandberg, A.; Nguyen, B. N.; Van Keuls, F. W.; Mueller, C. H.; Rodriguez-Solis, R.; Miranda, F. A. *ACS Appl. Mater. Interface* **2012**, *4*, 6346−6353.

(5) Rodriguez, O. R.; Cho, W.; Saxena, R.; Plawsky, J. L.; Gill, W. N. *J. Appl. Phys.* **2005**, *98*, 0241082.

(6) Koike, J.; Wada, M. *Appl. Phys. Lett.* **2005**, *87*, 0419114.

(7) International Technology Roadmap for Semiconductors Home Page. http://www.itrs.net/Links/2011ITRS/Home2011.htm (accessed Nov 11, 2012).

(8) Ganesan, P. G.; Singh, A. P.; Ramanath, G. *Appl. Phys. Lett.* **2004**, *85*, 579−581.

(9) Gandhi, D. D.; Lane, M.; Zhou, Y.; Singh, A. P.; Nayak, S.; Tisch, U.; Eizenberg, M.; Ramanath, G. *Nature* **2007**, *447*, 299−U2.

(10) Gandhi, D. D.; Tisch, U.; Singh, B.; Eizenberg, M.; Ramanath, G. *Appl. Phys. Lett.* **2007**, *91*, 14350314.

(11) Jain, A.; Singh, B.; Garg, S.; Ravishankar, N.; Lane, M.; Ramanath, G. *Phys. Rev. B* **2011**, *83*, 0354123.

(12) Rebiscoul, D.; Perrut, V.; Renault, O.; Rieutord, F.; Olivier, S.; Haumesser, P. H. *J. Supercrit. Fluid* **2009**, *51*, 287−294.

(13) Caro, A. M.; Armini, S.; Richard, O.; Maes, G.; Borghs, G.; Whelan, C. M.; Travaly, Y. *Adv. Funct. Mater.* **2010**, *20*, 1125−1131.

(14) Caro, A. M.; Maes, G.; Borghs, G.; Whelan, C. M. *Microelectron. Eng.* **2008**, *85*, 2047−2050.
(15) Davey, R. J.; Williams-Seton, L.; Lieberman, H. F.; Blagden, N. *Nature* **1999**, *402*, 797−799.
(16) Singh, B.; Garg, S.; Rathore, J.; Moore, R.; Ravishankar, N.; Interrante, L.; Ramanath, G. *ACS Appl. Mater. Inter.* **2010**, *2*, 1275−1280.
(17) Singh, B.; Hyun, J. Y.; Singh, A. P.; Gandhi, D.; Wu, Z.; Interrante, L. V.; Ramanath, G. *ACS Appl. Mater. Inter.* **2010**, *2*, 2180−2184.
(18) Garg, S.; Singh, B.; Liu, X. X.; Jain, A.; Ravishankar, N.; Interrante, L.; Ramanath, G. *J. Phys. Chem. Lett.* **2010**, *1*, 336−340.
(19) O'Brien, P. J.; Shenogin, S.; Liu, J. X.; Chow, P. K.; Laurencin, D.; Mutin, P. H.; Yamaguchi, M.; Keblinski, P.; Ramanath, G. *Nat. Mater.* **2013**, *12*, 118−122.
(20) Stoianov, S. V.; Daengngam, C.; Borhani, M.; Zhang, Y. F.; Morris, J. R.; Robinson, H. D. *ACS Appl. Mater. Interfaces* **2012**, *4*, 2348−2357.
(21) Chaudhari, M.; Du, J. C.; Behera, S.; Manandhar, S.; Gaddam, S.; Kelber, J. *Appl. Phys. Lett.* **2009**, *94*, 204102.
(22) Ding, Y. Z.; Garland, S.; Howland, M.; Revzin, A.; Pan, T. R. *Adv. Mater.* **2011**, *23*, 5551−5556.
(23) Aissaoui, N.; Bergaoui, L.; Landoulsi, J.; Lambert, J. F.; Boujday, S. *Langmuir* **2012**, *28*, 656−665.
(24) Oh, S. J.; Cho, S. J.; Kim, C. O.; Park, J. W. *Langmuir* **2002**, *18*, 1764−1769.
(25) Zhang, F. X.; Srinivasan, M. P. *Langmuir* **2004**, *20*, 2309−2314.
(26) Petersen, J.; Fouquet, T.; Michel, M.; Toniazzo, V.; Dinia, A.; Ruch, D.; Bomfim, J. *ACS Appl. Mater. Inter.* **2012**, *4*, 1072−1079.
(27) Worsley, M. A.; Bent, S. F.; Gates, S. M.; Fuller, N.; Volksen, W.; Steen, M.; Dalton, T. *J. Vac. Sci. Technol. B* **2005**, *23*, 395−405.
(28) Bailly, F.; David, T.; Chevolleau, T.; Darnon, M.; Posseme, N.; Bouyssou, R.; Ducote, J.; Joubert, O.; Cardinaud, C. *J. Appl. Phys.* **2010**, *108*, 0149061.
(29) Yin, Y. P.; Sawin, H. H. *J. Vac. Sci. Technol. A* **2008**, *26*, 151−160.
(30) Silverstein, M. S.; Shach-Caplan, M.; Khristosov, M.; Harel, T. *Plasma Process Polym.* **2007**, *4*, 789−796.
(31) Loscutoff, P. W.; Zhou, H.; Clendenning, S. B.; Bent, S. F. *ACS Nano* **2010**, *4*, 331−341.
(32) Yan, L.; Huck, W.; Zhao, X. M.; Whitesides, G. M. *Langmuir* **1999**, *15*, 1208−1214.
(33) Song, X. Y.; Zhai, J.; Wang, Y. L.; Jiang, L. *J. Colloid Interface Sci.* **2006**, *298*, 267−273.
(34) Cho, Y.; Ivanisevic, A. *J. Phys. Chem. B* **2004**, *108*, 15223−15228.
(35) Howarter, J. A.; Youngblood, J. P. *Langmuir* **2006**, *22*, 11142−11147.
(36) Chauhan, A. K.; Aswal, D. K.; Koiry, S. P.; Gupta, S. K.; Yakhmi, J. V.; Surgers, C.; Guerin, D.; Lenfant, S.; Vuillaume, D. *Appl. Phys. A: Mater.* **2008**, *90*, 581−589.
(37) Gambinossi, F.; Lorenzelli, L.; Baglioni, P.; Caminati, G. *Colloids Surf., A* **2008**, *321*, 87−93.
(38) Mikami, N.; Hata, N.; Kikkawa, T.; Machida, H. *Appl. Phys. Lett.* **2003**, *83*, 5181−5183.
(39) Lane, M.; Dauskardt, R. H.; Krishna, N.; Hashim, I. *J. Mater. Res.* **2000**, *15*, 203−211.
(40) Gandhi, D. D.; Singh, B.; Singh, A. P.; Moore, R.; Simonyi, E.; Lane, M. W.; Ramanath, G. *J. Appl. Phys.* **2009**, *106*, 0545025.
(41) Xiao, S. J.; Textor, M.; Spencer, N. D.; Sigrist, H. *Langmuir* **1998**, *14*, 5507−5516.
(42) Sugimura, H.; Moriguchi, T.; Kanda, M.; Sonobayashi, Y.; Nishimura, H. M.; Ichii, T.; Murase, K.; Kazama, S. *Chem. Commum.* **2011**, *47*, 8841−8843.
(43) Han, L.; Pan, J. S.; Chen, S. M.; Balasubramanian, N.; Shi, J. N.; Wong, L. S.; Foo, P. D. *J. Electrochem. Soc.* **2001**, *148*, F148−F153.
(44) Millet, B.; Fiaud, C.; Hinnen, C.; Sutter, E. *Corros. Sci.* **1995**, *37*, 1903−1918.
(45) Gandhi, D. D.; Singh, A. P.; Lane, M.; Eizenberg, M.; Ramanath, G. *J. Appl. Phys.* **2007**, *101*, 0845058.
(46) Baio, J. E; Weidner, T.; Brison, J.; Graham, D. J.; Gamble, L. J.; Castner, D. G. *J. Electron Spectrosc.* **2009**, *172*, 2−8.
(47) Wang, H.; Chen, S. F.; Li, L. Y.; Jiang, S. Y. *Langmuir* **2005**, *21*, 2633−2636.
(48) Sprik, M.; Delamarche, E.; Michel, B.; Rothlisberger, U.; Klein, M. L.; Wolf, H.; Ringsdorf, H. *Langmuir* **1994**, *10*, 4116−4130.
(49) Biemolt, W.; Jansen, A.; Neurock, M.; Vandekerkhof, G.; Vansanten, R. A. *Surf. Sci.* **1993**, *287*, 183−187.
(50) D'Souza, A. S.; Pantano, C. G. *J. Am. Ceram. Soc.* **2002**, *85*, 1499−1504.
(51) Lee, Y. S. *Self-Assembly and Nanotechnology: A Force Balance Approach*; John Wiley & Sons: Hoboken, NJ, 2008.
(52) Lane, M. W.; Snodgrass, J. M.; Dauskardt, R. H. *Microelectron. Eng.* **2001**, *41*, 1615−1624.